

Influence of solvent quality on effective pair potentials between polymers in solution

V. Krakoviack*, J.-P. Hansen, and A. A. Louis
*Department of Chemistry, University of Cambridge,
 Lensfield Road, Cambridge CB2 1EW, United Kingdom*
 (Dated: March 11, 2021)

Solutions of interacting linear polymers are mapped onto a system of “soft” spherical particles interacting via an effective pair potential. This coarse-graining reduces the individual monomer-level description to a problem involving only the centers of mass (CM) of the polymer coils. The effective pair potentials are derived by inverting the CM pair distribution function, generated in Monte Carlo simulations, using the hypernetted chain (HNC) closure. The method, previously devised for the self-avoiding walk model of polymers in good solvent, is extended to the case of polymers in solvents of variable quality by adding a finite nearest-neighbor monomer-monomer attraction to the previous model and varying the temperature. The resulting effective pair potential is found to depend strongly on temperature and polymer concentration. At low concentration the effective interaction becomes increasingly attractive as the temperature decreases, eventually violating thermodynamic stability criteria. However, as polymer concentration is increased at fixed temperature, the effective interaction reverts to mostly repulsive behavior. These issues help illustrate some fundamental difficulties encountered when coarse-graining complex systems via effective pair potentials.

I. INTRODUCTION

While the computer simulation of single, isolated polymer chains, either on or off lattice, using a variety of conformation sampling algorithms, is nowadays relatively routine, for up to $L \simeq 10^6$ monomers or segments [1], it is computationally much more demanding to simulate polymer solutions or melts, involving large numbers of interacting polymer chains. Indeed, if N is the number of such chains and L the number of segments per polymer, then the total number of interacting particles, NL , can become very large, particularly so if L is sufficiently large for the scaling regime to be reached [2]. Under these conditions it is tempting to seek a coarse-graining procedure to reduce the full segment-level description to a model involving only the center of mass (CM) or the central monomer of each chain, thus reducing the initial NL -body problem to a N -body problem. This is formally achieved by tracing out the individual monomer degrees of freedom, i.e. by averaging over polymer conformations for fixed positions of the CM’s or central monomers of interacting polymer coils, taking into account the appropriate Boltzmann weights. This idea goes back to Flory and Krigbaum [3]. They predicted that the effective repulsive interaction between the CM’s of linear self-avoiding walk (SAW) polymers should diverge with molecular weight at full overlap, i.e. when the CM’s of the two coils coincide. It was first realized by Grosberg *et al.* [4] that in fact the pair potential between CM’s remains finite in the scaling limit $L \rightarrow \infty$, and of the order of a few $k_B T$, reflecting the purely entropic origin of the effective interaction. The effective CM pair potential between two isolated SAW polymer coils was explicitly

evaluated by Monte Carlo (MC) simulations of on and off-lattice models [5, 6, 7], and by renormalization group (RG) calculations [8]. These studies show that the effective pair potential is purely repulsive, with an overlap (zero separation) value of about $2k_B T$ and a range of the order of the radius of gyration R_g . The zero concentration pair potential is reasonably well represented by a single Gaussian of width R_g .

More recently the effective pair potential was determined at *finite* polymer concentration by a combination of monomer-level MC simulations of lattice SAW polymers, and an inversion technique based on integral equations for pair distribution functions in simple liquids [9]. The resulting pair potentials depend now moderately on polymer concentration [7, 10], but they remain essentially repulsive and of range R_g . They have been put to good use to reproduce the interfacial tension of semi-dilute polymer solutions near hard walls or colloidal spheres [11], and to determine the depletion interaction between colloidal particles induced by interacting (rather than ideal) polymer coils [12] and the resulting, depletion-induced phase diagram of colloidal dispersions [13].

The present paper reports an extension of the above inversion strategy to the case of dilute and semi-dilute solutions of interacting linear polymers in solvents of variable quality, spanning the range between good solvent conditions, modeled by the SAW, and poor solvent conditions, where the coils contract to avoid contact with the solvent. This generalization is achieved by adding a finite attractive interaction between nearest-neighbor monomers of the same or different chains, while maintaining infinite repulsion between overlapping monomers. The finite nearest-neighbor attraction introduces an energy scale, and hence a temperature dependence of the effective pair potential. Good solvent conditions correspond to the infinite temperature limit, leading back to the SAW model considered earlier, while increasingly

*Present address: Laboratoire de Chimie, École Normale Supérieure de Lyon, 46, Allée d’Italie, 69364 Lyon Cedex 07, France.

poor solvent conditions are mimicked by enhancing the attraction between monomers, or equivalently, decreasing the temperature.

The dependence of the properties of a single polymer coil, like its radius of gyration R_g , on temperature, and in particular around and below the θ temperature where the coil to globule transition takes place, has been studied by extensive MC simulations of very long chains (L up to 10^6) by Grassberger and collaborators [14]. Results for the temperature dependence of the effective pair potential for an off-lattice model of two polymer coils (i.e. in the infinite dilution limit) were reported by Dautenhahn and Hall [6]. These authors met with increasing MC sampling difficulties as the temperature is decreased towards the θ point. The present paper improves on their results by considering a lattice model, and using an overlapping distribution method [15, 16] to sample rare conformations which become increasingly important as the temperature decreases. The main objective of this paper is to consider, for the first time, the effective pair potential between the CM's of polymer coils in poor solvent at *finite* polymer concentration, i.e. to investigate both the temperature and concentration dependence of the CM pair potential, in particular in the vicinity of the θ point. The polymer model studied in this work is defined in Section II. The zero concentration limit is first considered in Section III, while finite polymer concentrations are examined next in Section IV. Some considerations on the use of effective interactions in relation to thermodynamic stability are presented in Section V, and conclusions are drawn in Section VI.

II. MODEL AND BASIC PHENOMENOLOGY

For all the calculations in the present work, a lattice model defined on the simple cubic lattice (with a coordination number of six) was used [17]. A polymer chain of length L is represented as a connected sequence of L lattice sites. The monomers, defined as occupied sites, interact with each other via excluded volume repulsion, preventing two of them from occupying the same lattice position, and lattice nearest-neighbor attraction $\varepsilon < 0$ between non-bonded pairs of monomers. For convenience, the temperature T will be expressed in units of $-\varepsilon/k_B$, or equivalently we will set $\varepsilon = -1$ and $k_B = 1$. With this convention, the usual β appearing in the Boltzmann factor is simply the inverse of the temperature, i.e. $\beta = 1/T$. In the following, we shall call “contact” any nearest-neighbor pair of non-bonded monomers. We use “intramolecular” if both monomers belong the same chain, and “intermolecular” otherwise. When a system consisting of N chains of L segments is considered on a portion of cubic lattice of M sites, the monomer packing fraction is equal to the fraction of lattice sites occupied by polymer segments, $c = NL/M$, while the concentration of polymer chains is $\rho = c/L = N/M$.

This simple model has been extensively studied in

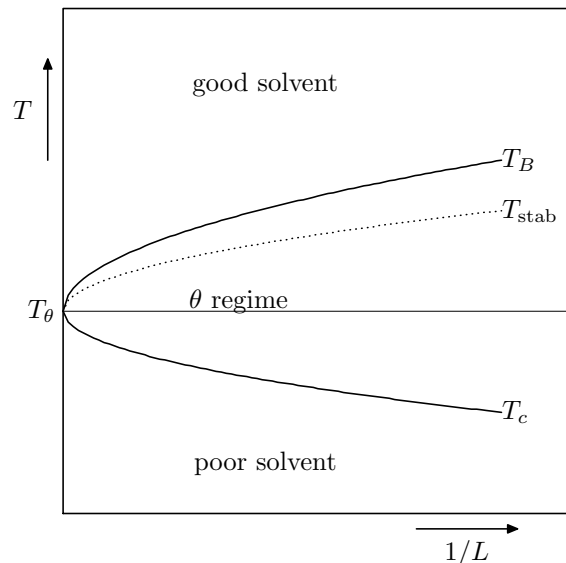


FIG. 1: Schematic temperature-inverse length diagram showing the three regimes of polymer phenomenology and the behavior of the temperatures T_θ , T_B , T_{stab} , and T_c (defined in the text) related to the characterization of the θ regime.

order to investigate the properties of isolated polymer chains and of polymer solutions. In the phenomenology of these systems, three different domains, sketched on Fig. 1, are usually defined, corresponding to different behaviors of an isolated chain.

In the good solvent regime, corresponding in the present model to high temperatures, the properties of the system are essentially determined by the entropic effects originating in connectivity and excluded volume interactions. An isolated chain takes swollen coil configurations with a radius of gyration R_g known to scale as L^ν , where $\nu \simeq 0.588$ is the Flory exponent in three dimensions [18]. This regime has been extensively studied in the case of the SAW to which the present model reduces in the infinite temperature limit [19].

In the bad or poor solvent regime, corresponding here to low temperatures, entropic effects are overwhelmed by the attractive monomer-monomer interactions and a chain molecule collapses into a compact globule with a radius of gyration scaling like $L^{1/3}$.

Between these two extremes lies the θ regime, where energetic and entropic effects compensate each other. In this regime, in the limit of infinite length, a chain has the scaling properties of an ideal chain, for instance $R_g \propto L^{1/2}$. The characterization of this domain has been the focus of many studies using the present lattice model [20, 21, 22, 23], with in particular extensive work by Grassberger and coworkers [14, 24, 25].

Of key importance is the so-called θ temperature, T_θ , at which the tricritical coil-to-globule transition takes place for an isolated chain in the $L \rightarrow \infty$ limit. It corresponds to a real thermodynamic singularity and its best

estimate is presently [24]

$$T_\theta = 3.717 \pm 0.003, \text{ i.e. } \beta_\theta = 0.2690 \pm 0.0002.$$

Obviously, simulations can only deal with chains of finite length, for which the tricritical singularity is rounded off by significant finite size corrections. T_θ is thus not directly accessible and it is common practice, in simulations as well as in experiments, to obtain it by extrapolation of related, length-dependent characteristic temperatures.

The most widely used of such temperatures is Boyle's temperature, $T_B(L)$, defined as the temperature at which the osmotic second virial coefficient of chains of length L vanishes. From its knowledge, one can compute the θ temperature from the limit

$$\lim_{L \rightarrow \infty} T_B(L) = T_\theta. \quad (1)$$

This route has been followed in particular in Ref. [14], where it was found that $T_B(L)$ is always greater than T_θ and decreases with increasing L .

An alternative possibility is to use the demixing critical temperature of the polymer solution. This marks the limit between a high temperature regime where the chains in solution form a homogeneous fluid, and a low temperature domain where the chains start to coagulate and the fluid demixes into polymer-rich and polymer-poor phases. In the lattice model used here, where the solvent is taken into account implicitly through the introduction of constant attractive monomer-monomer interactions and variations of the temperature, it is simply the critical temperature $T_c(L)$ of the liquid-gas transition of the system. As for $T_B(L)$, one has

$$\lim_{L \rightarrow \infty} T_c(L) = T_\theta, \quad (2)$$

and it has been found in Refs. [23] and [25] that $T_c(L)$ is always smaller than T_θ and increases with increasing L .

We anticipate on the following sections and introduce here a third characteristic temperature called the "stability" temperature and denoted $T_{\text{stab}}(L)$. It is associated with a fundamental breakdown in the statistical-mechanical treatment of the coarse-grained effective pair interaction $v_2(r)$ between the CM's of two polymer chains at low temperature. Singularities of a similar nature have been encountered in various models for soft matter systems. For instance, Baxter's sticky sphere model [26] displays anomalous clustering towards a closed-packed crystalline phase as a result of breakdown of thermodynamic stability [27]. In the case of polymers, the Domb-Joyce model [28] shows self-trapping behavior, i.e. a chain remains of finite extent in the infinite length limit, when a negative energy is attributed to self-crossings [29].

The relation between $T_{\text{stab}}(L)$ and the θ point is unclear. For any length L , $T_{\text{stab}}(L)$ will be shown to be smaller than $T_B(L)$, the equality being only achieved when the pair interaction is zero. For the specific length $L = 100$ studied in detail in this paper, it is found to fall between $T_B(L)$ and T_θ . Because it corresponds to

a singularity in the statistical-mechanical treatment of the system, it is tempting to assume, as it was done in Ref. [30], that

$$\lim_{L \rightarrow \infty} T_{\text{stab}}(L) = T_\theta, \quad (3)$$

and Fig. 1 has been drawn under this assumption. Interestingly, this would imply that, in the infinite length limit, since $T_B(L \rightarrow \infty) = T_{\text{stab}}(L \rightarrow \infty) = T_\theta$, the effective interaction between two isolated polymer chains at the θ point vanishes identically for all distances, a behavior which is trivially found in the case of the Domb-Joyce model [28], when a positive constant energy penalty is counted for each polymer crossing (note that in this model, the temperature scale is reversed since the SAW is obtained at zero temperature and ideal chain behavior is found at infinite temperature).

III. ZERO DENSITY LIMIT

A. Simulation methodology

In the zero density limit, the effective interaction potential $v_2(r)$ between two polymer chains is equal to the difference between the free energy of the two chains with their centers of mass constrained to stay at a fixed distance r , and the free energy of the same chains infinitely far apart. It can be expressed as follows.

Consider two polymer chains labeled A and B . When these chains have conformations Γ_A and Γ_B respectively, with the vector \mathbf{r}_{AB} joining their centers of mass, the energy of the pair is

$$H(\mathbf{r}_{AB}; \Gamma_A, \Gamma_B) = H_{\text{intra}}(\Gamma_A) + H_{\text{intra}}(\Gamma_B) + H_{\text{inter}}(\mathbf{r}_{AB}; \Gamma_A, \Gamma_B), \quad (4)$$

where the intra- and intermolecular parts (including the hard-core interactions) have been separated. Introducing the intermolecular Boltzmann weight

$$W(|\mathbf{r}_{AB}|; \Gamma_A, \Gamma_B) = \exp[-\beta H_{\text{inter}}(\mathbf{r}_{AB}; \Gamma_A, \Gamma_B)], \quad (5)$$

the effective pair potential is given by [31]

$$\beta v_2(r) \equiv -\ln \langle W(|\mathbf{r}_{AB}| = r; \Gamma_A, \Gamma_B) \rangle, \quad (6)$$

where the brackets denote an average over the probability distribution of two isolated chains, which is the square of the probability distribution \mathcal{P} of a single chain, i.e.

$$\langle W(|\mathbf{r}_{AB}| = r; \Gamma_A, \Gamma_B) \rangle = \sum_{\Gamma_A, \Gamma_B} \mathcal{P}(\Gamma_A) \mathcal{P}(\Gamma_B) W(|\mathbf{r}_{AB}| = r; \Gamma_A, \Gamma_B) \quad (7)$$

with

$$\mathcal{P}(\Gamma) = \exp[-\beta H_{\text{intra}}(\Gamma)] \left/ \sum_{\Gamma} \exp[-\beta H_{\text{intra}}(\Gamma)] \right. . \quad (8)$$

This result provides us with a direct means to compute the effective pair potential between two chains by Monte Carlo simulations. We sample configurations of two independent chains using the pivot algorithm [32] and standard Metropolis acceptance rules. The latter ensure that the chain conformations are generated according to the probability distribution \mathcal{P} . After every 1000 pivot moves for each chain, we calculate the intermolecular Boltzmann weight (5) as a function of the CM distance, by moving the polymers towards each other, while checking for overlap and counting intermolecular contacts. Eventually, $\beta v_2(r)$ is obtained by performing the unweighted average of $W(|\mathbf{r}_{AB}| = r; \Gamma_A, \Gamma_B)$ on the sample considered:

$$\beta v_2(r) = -\ln \frac{\sum_{i=1}^{\mathcal{N}(r)} W(|\mathbf{r}_{AB}| = r; \Gamma_A^i, \Gamma_B^i)}{\mathcal{N}(r)}, \quad (9)$$

where $\mathcal{N}(r)$ is the number of two chain configurations with CM's at distance r sampled during the simulation.

Using this algorithm, we have been able to compute with good statistical accuracy effective pair potentials for various chain lengths ($L = 100, 200$ and 500), provided $\beta \leq 0.2$.

Unfortunately, this simple, direct method turns out to be inadequate at lower temperatures, where the results for the effective potential at short distances are found to fluctuate strongly with the sample considered, with no significant reduction of the corresponding statistical uncertainties when the size of this sample is increased. The origin of this problem, already seen in the analogous off-lattice calculation of Dautenhahn and Hall [6], has been carefully analyzed by Grassberger and Hegger in their calculation of the second virial coefficient of the same lattice model as the one studied here [14]. At low temperature, the polymer chains start to collapse significantly and are thus rather compact. This means that at short distances, most two-chain configurations obtained with the present direct algorithm will overlap and the corresponding intermolecular Boltzmann weights are then identically zero. But, in the rare cases where the two chains do not overlap, many contacts will usually be formed, leading to very low negative intermolecular energies and thus huge intermolecular Boltzmann weights contributing to the pair potential. The need to average such unevenly distributed numbers of very different amplitudes gives rise to the large observed fluctuations and renders the direct approach useless.

Hence more elaborate algorithms must be used for low temperatures. In order to choose these new tools, it is helpful to recognize the strong similarity between the previous scheme and Widom's particle insertion method for the computation of the chemical potential [33]. Both methods indeed involve the averaging of a Boltzmann weight over the equilibrium distribution of some unperturbed system, and in fact the observed breakdown of the direct calculation of the effective pair potential at low

temperature parallels that of Widom's method at high fluid densities. In the latter case, an efficient approach to solve the problem has been devised by Shing and Gubbins [34], which belongs to the general class of overlapping distribution methods first introduced by Bennett to compute free-energy differences [15, 16]. We have thus implemented such a method which is described in detail in the Appendix.

Using this histogram method, we have been able to extend our calculation of the effective pair potentials between chains of length $L = 100$ to lower temperatures, i.e. up to $\beta = 0.3$. However, the method breaks down when applied to longer chains, for mainly two reasons. Firstly, the acceptance ratio of the elementary Monte Carlo move becomes extremely small, leading to serious ergodicity problems in the simulations. Secondly, except for small separations corresponding to nearly complete overlap of the chains, the two computed histograms do not overlap at all, rendering the estimation of the required free energy difference quite problematic. The origin of this problem can easily be understood on a qualitative level. In the original system, the chains attract each other strongly and lower their intermolecular energy at low temperature by elongating towards each other along the axis joining their CM's: there is thus a sizeable volume where the two chains overlap with the consequent formation of contacts in large numbers [35]. On the contrary, in the reference system, only unfavorable excluded volume interactions exist between the two partly collapsed chains which are thus compressed along the axis joining their CM's to limit their overlap [6]: contacts are then formed in small numbers only at the surface separating the two segregated chains. This significant separation in the number of contacts does not occur (or at least is less pronounced for the lengths studied here) at complete overlap because the system has then to keep the spherical symmetry of the isolated chains, thus leaving no possibility for the adverse changes of the chain shapes seen in the cylindrical symmetry.

Although it would be possible to use alternative methods (see e.g. [14, 23]) to sample even longer chains at low temperature, we use mainly $L = 100$ chains in this paper, since we do not expect the qualitative features we focus on here to depend strongly on chain length [36]. Of course, quantitative features will vary with L , and the detailed scaling behavior can be quite complex [24, 25].

B. Results

The effective pair interactions $\beta v_2(r)$ between two polymers of length $L = 100$ are plotted, for various solvent qualities, in Fig. 2. The product of the potential by $4\pi r^2$ is shown as well, because the integral of this quantity plays an important role for the thermodynamics of the system [30, 37], and to emphasize the features of the potential at large distances. In this figure and in all the following figures representing effective pair potentials, all

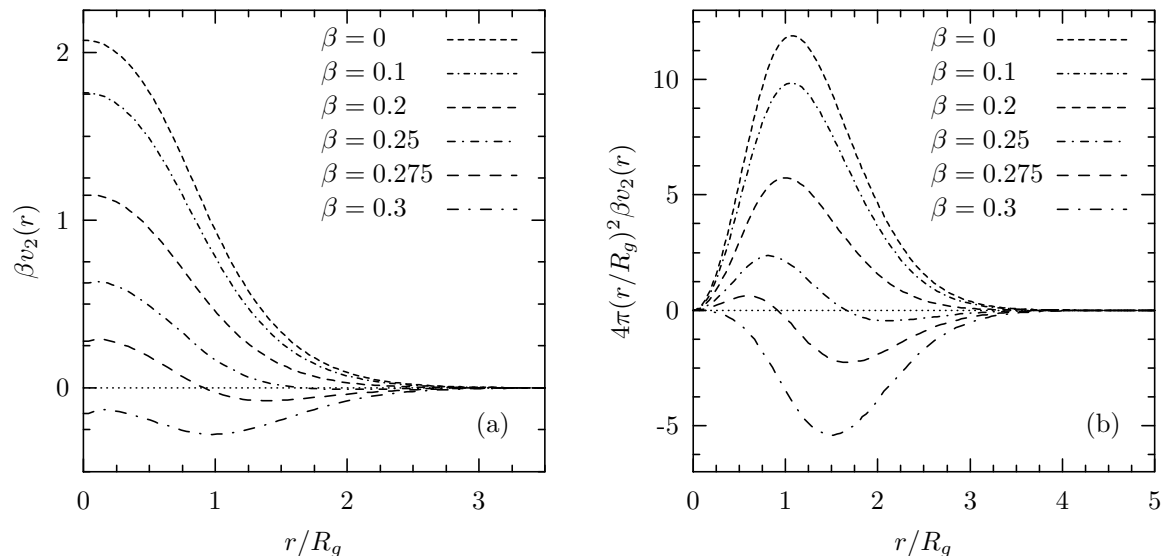


FIG. 2: Zero density effective pair potentials at different inverse temperatures β for polymers of length $L = 100$ on the simple cubic lattice. At each temperature, the x -axis is scaled with the corresponding $R_g(\beta)$, which is shown in Fig. 3

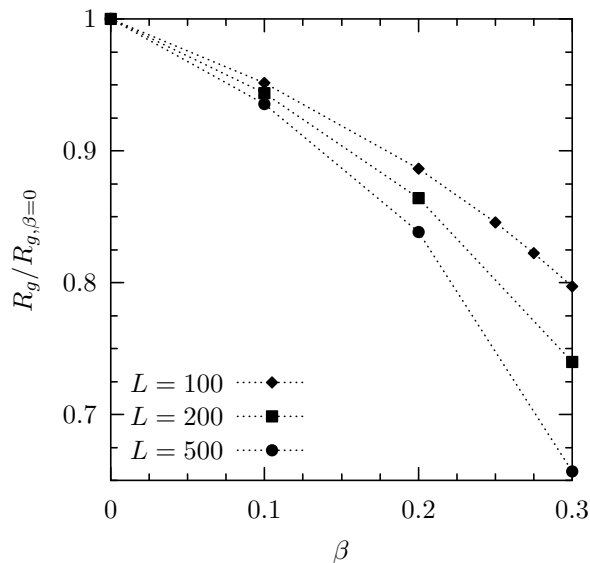


FIG. 3: Radii of gyration of isolated polymer chains of different lengths L on the simple cubic lattice as functions of the inverse temperature β . The data are scaled with the infinite temperature values, $R_g(L = 100) = 6.44$, $R_g(L = 200) = 9.76$, and $R_g(L = 500) = 16.84$.

distances have been scaled at each temperature by the radius of gyration of the isolated chain at this temperature, which is plotted in Fig. 3 for completeness.

One can distinguish two temperature domains. In Ref. [7], where the infinite temperature limit of the model was studied, $\beta v_2(r)$ was found to be purely repulsive with a roughly Gaussian shape centered on $r = 0$. Here we find that it remains so, provided the temperature is high enough, i.e. $\beta \lesssim 0.2$. The main effect of lowering the

temperature is a reduction of the overall amplitude of the potential and a slight decrease in its range in terms of the normalized distance.

At lower temperatures, $\beta > 0.2$, $\beta v_2(r)$ begins to exhibit qualitative changes: while the potential retains a repulsive Gaussian-like component at short distance, a negative, attractive tail appears at large distance. As the temperature decreases further, the amplitude of the repulsive core decreases, following the trend of the previous high temperature domain, whereas the attractive tail becomes more and more important, ultimately dominating the whole picture, as seen for $\beta = 0.3$, where $\beta v_2(r)$ is everywhere negative and only a modest repulsion shows up for $r/R_g < 1$.

A second, less prominent feature appears at low temperature ($\beta \gtrsim 0.2$) as well. At $r = 0$, the effective pair potential displays a small minimum, which becomes deeper when the temperature decreases. This means that full overlap is locally stable and that one has to overcome a (modest) free-energy barrier to separate two chains in this configuration. For chains of length $L = 100$, it is difficult to know if this feature is a generic property of the effective pair potential or just a lattice artifact due to the shortness of the chains (the width of the minimum is indeed of the order of the lattice spacing). However, despite our limited ability to investigate longer chains at low temperature, we have seen evidence of a similar minimum, but of larger width, for chains of length $L = 500$ at $\beta = 0.225$, suggesting that this is a genuine physical effect.

One can compute various interesting scalar quantities from the knowledge of the effective pair potential. According to Sec. II, the second osmotic virial coefficient,

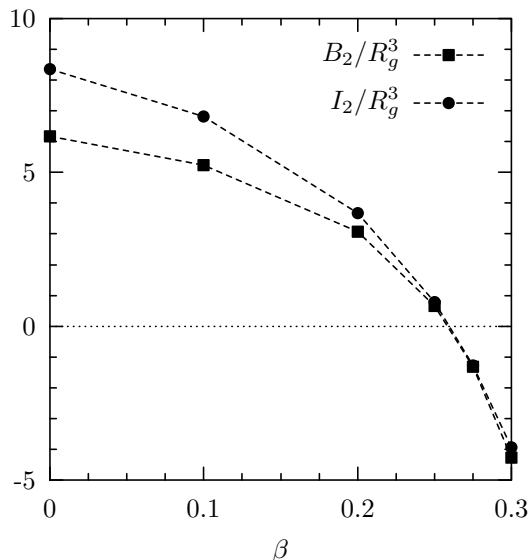


FIG. 4: Reduced second osmotic virial coefficient (B_2/R_g^3) and reduced stability integral at zero density (I_2/R_g^3) as functions of the inverse temperature β for polymers of length $L = 100$ on the simple cubic lattice.

given by

$$B_2(\beta) = \frac{1}{2} \int_0^\infty [1 - \exp(-\beta v_2(r))] 4\pi r^2 dr, \quad (10)$$

is of particular importance. In addition, we introduce the “stability” integral,

$$I_2(\beta) = \frac{1}{2} \int_0^\infty \beta v_2(r) 4\pi r^2 dr, \quad (11)$$

which results from the linearization of the exponential in Eq. (10). For systems interacting through *density-independent* potentials, the sign of I_2 gives a necessary condition for the existence of the thermodynamic limit and the stability of the system against coalescence [38, 39], as will be further developed in Sec. V. Accordingly, as discussed by anticipation in Sec. II, a “stability” temperature $T_{\text{stab}}(L)$ can be defined, at which $I_2(\beta)$ vanishes for chains of length L , and below which the necessary condition for stability against coalescence is violated. The ordering $T_{\text{stab}}(L) \leq T_B(L)$ discussed above is then an immediate consequence of the fact that $x \geq 1 - \exp(-x)$.

Both quantities, normalized with the cube of the radius of gyration to obtain dimensionless quantities, are plotted in Fig. 4. As was implicitly assumed above, they are decreasing functions of β and one finds, for the chains of length $L = 100$ studied here, that $T_B \gtrsim T_{\text{stab}} \simeq 3.8$.

Finally, we address the question of the dependence of the zero density effective pair potential on the chain length. In Ref. [7], the infinite temperature case has been studied in detail over a wide range of polymer lengths ($L = 100$ to 8000). Such an extensive study was not attempted here and we only considered two rather short

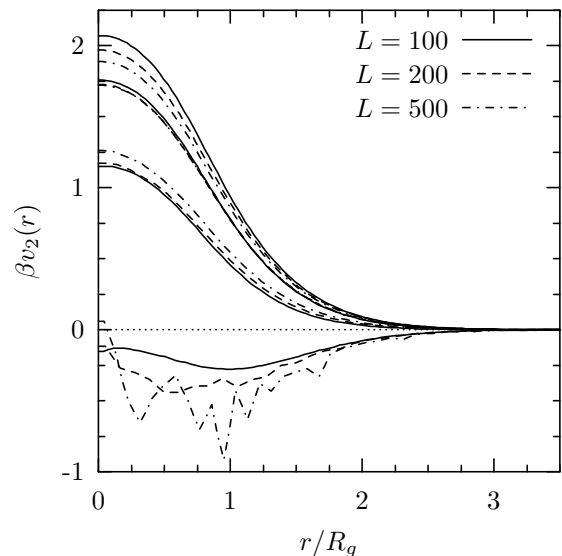


FIG. 5: Zero density effective pair potentials at different inverse temperatures β (from top to bottom, for a given length, $\beta = 0, 0.1, 0.2,$ and 0.3) for polymers of various lengths L on the simple cubic lattice. At each temperature, the x -axis is scaled with the corresponding $R_g(\beta)$.

lengths ($L = 200$ and 500) in addition to the previous data for $L = 100$. All these data, plotted in Fig. 5 with the one previously described, have been computed with the direct method, leading to strong statistical uncertainties at the lowest temperature corresponding to $\beta = 0.3$.

To interpret these potentials one should keep in mind that R_g scales differently with temperature for the different lengths, as illustrated in Fig. 3. Also, T_B and T_C are different for each length. Following Refs. [14] and [25], in which these temperatures have been computed with great care, for $L = 100$: $T_C \simeq 3.10$; $T_B \simeq 3.86$; for $L = 200$: $T_C \simeq 3.33$; $T_B \simeq 3.81$; for $L = 500$: $T_C \simeq 3.41$; $T_B \simeq 3.77$.

A few qualitative observations can be made, at least for $\beta \leq 0.2$, where the statistics are good enough. With the normalization chosen for the x -axis, no intersection between potentials corresponding to different values of L at the same temperature is found. In Ref. [7], this feature was already found for $\beta = 0$, combined with the fact that a larger L leads to a less repulsive potential. We recover this result here and the same qualitative behavior is found for $\beta = 0.1$, but the potentials for different values of L are closer. This behavior changes for $\beta = 0.2$, where we now see that the larger L , the more repulsive the potential. Globally, we thus find that in the high-temperature domain, the decrease in the amplitude of the repulsive effective potential is slower for large values of L .

It is difficult to draw conclusions from the data at $\beta = 0.3$, but it looks like the larger L , the deeper the attractive potential. Indeed, for large CM distances, at which the statistical inaccuracies in the simulation results are

expected to be modest, the potential seems to be more negative when L is large; the same holds at complete overlap: trying to estimate $\beta v_2(0)$ for $L = 500$ with the overlapping distribution method, we find $\beta v_2(0) \simeq -1.1$, to be compared to $\beta v_2(0) \simeq -0.15$ for $L = 100$.

All these results, if applied to Eq. (10), are consistent with the findings of Grassberger and Hegger for the variation of the reduced second osmotic virial coefficient, B_2/R_g^3 , with temperature for various lengths (see Fig. 16 in Ref. [14]). Indeed, they found that the larger L , the flatter this quantity is in the high temperature regime, the more abrupt the downward bend of the curve when approaching $T_B(L)$ and the faster the divergence towards $-\infty$ in the poor solvent regime.

IV. FINITE DENSITIES

A. Methodology

Having derived the effective potential between two isolated polymers, we now turn to polymers at finite density. For this, we follow the route proposed in previous work [7], in which an effective pair potential was constructed to exactly reproduce the two-body CM correlations of the full underlying many-body system. In fact, it can be proven for a wide variety of systems that for any given pair distribution function $g(r)$ at given inverse temperature β and density ρ , there exists a corresponding unique two-body pair potential $v(r)$ which reproduces $g(r)$ irrespective of the underlying many-body interactions in the system [40]. Of course, $g(r)$ depends on density and temperature and contains contributions not only from the bare pair potential $v_2(r)$, but also from the three- and more-body terms. As a consequence, the effective pair interaction will also be state dependent and a new effective potential, hereafter denoted $v(r; \rho, \beta)$, must be calculated for each density and temperature. However this inversion approach says nothing about a possible volume term $v_1(\rho, \beta)$, in the coarse-grained total potential energy, which contributes to the equation of state, but not *directly* to the pair-correlations [41, 42]. Of course the volume terms may still contribute *indirectly*, for example when they induce phase transitions.

The inversion procedure, using $g(r)$ to extract $v(r)$, is well known and has been studied extensively in the field of simple fluids [43, 44]. We invert $g(r)$ using the hypernetted chain (HNC) closure,

$$g(r) = \exp(-\beta v(r) + g(r) - c(r) - 1), \quad (12)$$

of the Ornstein-Zernike equation [9]. While the simple HNC inversion procedure would be inadequate for dense fluids of hard core particles, where more sophisticated closures or iterative procedures are required [43, 44], we are able to demonstrate the consistency of the HNC inversion in the present case.

To compute the necessary structural information we have performed canonical Monte Carlo simulations of

polymer solutions. We have studied chains of length $L = 100$ in a cubic box of size $M = 100^3$ with periodic boundary conditions, varying the number of polymers from $N = 400$ to $N = 3200$ ($c = 0.04$ to 0.32). Four temperatures have been considered corresponding to $\beta = 0, 0.1, 0.2$, and 0.3 . Note that the lowest temperature, $T = 3.33$, is slightly larger than the critical temperature of the system, $T_c(L = 100) \simeq 3.1$ according to Ref. [25], thereby avoiding concerns with the possible two-phase behavior of the system. To sample the configuration space of the system we have used standard techniques of polymer simulations: pivot moves [32], translation moves, and, for high densities where the previous moves become inefficient, configurational bias Monte Carlo (CBMC) moves, in which an extremity or part of the interior of a chain are regrown [16].

In the course of the simulations, the CM of each polymer was tracked in order to construct the CM radial pair distribution function $g(r; \beta, \rho)$. The latter is only known up to a cutoff radius r_c , which corresponds to half the size of the simulation box. For the inversion, we need $g(r)$ for all r , so we employ the following iterative scheme to extend $g(r)$. As an initial step, we set $g(r) = 1$ for $r > r_c$ and calculate the corresponding $v(r)$ by inversion. We then set $v(r) = 0$ for $r > r_c$ and determine the corresponding $g(r)$ for $0 < r < \infty$ by a regular HNC calculation, using a simple iterative procedure. The $g(r)$ for $r < r_c$ is then replaced by the measured $g(r)$, and the new $v(r)$ is calculated. This is again set to zero for $r > r_c$, and the process is repeated until convergence. In fact, because of the finite box-size, the inversion process is underdetermined, and our ansatz that $v(r) = 0$ for $r > r_c$ is needed to find a unique solution [10]. This is not unreasonable since we do not expect the interactions between the polymer coils to be significant beyond distances a few times the radius of gyration. However, to make sure that this is actually the case, we found that relatively large simulation boxes were needed, with a lattice size of up to $10\text{-}15R_g$. This is particularly important at high density, where the inverted potential becomes longer ranged and more sensitive to small changes in the radial distribution function $g(r)$. In all our inversions, we checked explicitly that $v(r)$ becomes effectively zero before $r = r_c$, confirming our initial ansatz.

B. Results

Before presenting the results for the effective pair potentials, we first discuss briefly the behavior of the radius of gyration with density and temperature, which is an important measure of the physical properties of the polymer. The corresponding simulation data are plotted in Fig. 6. As found in similar previous work [45], for a given temperature, R_g decreases when the density of polymer increases if this temperature falls into the good solvent regime, whereas R_g increases if this temperature is located below the θ regime (Fig. 6a). When R_g is plot-

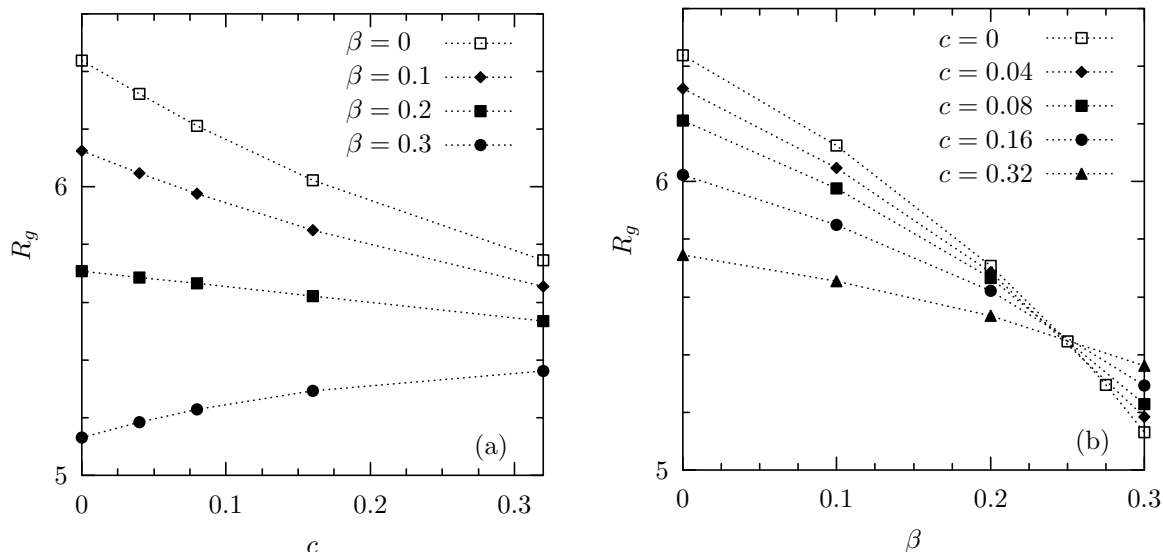


FIG. 6: Density- and temperature-dependence of the radius of gyration of polymers of length $L = 100$ on the simple cubic lattice. (a) Radii of gyration as functions of the monomer density c for various inverse temperatures β . (b) Radii of gyration as functions of the inverse temperature β for various monomer densities c .

ted as a function of temperature for various densities, this results in the existence of a regime, located in the θ region, where R_g is nearly independent of c , as can be seen in Fig 6b, where all the curves are seen to converge around $\beta \simeq 0.25$.

The effective temperature- and density-dependent pair potentials are plotted in Figs. 7 and 8 for two representative temperatures, corresponding to $\beta = 0.1$ and $\beta = 0.3$ respectively. From these data, it is clear that the two temperature domains identified in the zero density study of Sec. III display obvious distinctive features in terms of the density dependence of the effective pair potentials at fixed temperature.

When $\beta = 0.1$ (Fig. 7), i.e. in the high temperature regime, a moderate density dependence is found. Starting from the purely repulsive, nearly Gaussian shape of the potential at zero density and increasing the density, one finds a slight increase in the amplitude and in the range of the repulsive potential for small separations of the polymer CM's and the progressive appearance of a weak negative attractive tail at large distance. This behavior is similar to the one found in the infinite temperature limit studied in Ref. [7], with the only minor difference that we do not see a decrease of the amplitude of the potential at short distances for the highest concentrations.

The situation is completely different when $\beta = 0.3$ (Fig. 8). Here the density dependence of the effective pair potential is very important and leads to significant qualitative changes in the shape of the potential: whereas at low density, $v(r)$ is negative and essentially attractive, repulsion between centers of mass progressively builds up when the density increases, so that an almost purely repulsive, Gaussian shaped $v(r)$ is eventually observed

at the largest density. For the good solvent case a clear link has been found between the density dependence and the strength of the 3- and higher body interactions [46, 47]. Presuming that the same link can be made here, this would imply that the many-body interactions are relatively more important at lower temperatures.

The virial coefficient has no clear interpretation for potentials obtained at finite global densities, whereas the “stability” integral does still define a lower limit to the existence of a thermodynamic limit of the coarse-grained system. As can be directly seen from Fig. 8b, at all densities, except the largest ($c = 0.32$), the stability integral of the computed potentials is negative, leading to serious consistency issues to be discussed in the next section.

V. CONSIDERATIONS OF THERMODYNAMIC STABILITY

The potentials computed in this work raise a number of interesting conceptual issues with regard to the use of effective potentials in coarse-grained descriptions of material properties. The first question concerns *thermodynamic stability* [38]: do the calculated pair potentials generate a valid thermodynamic limit? Secondly, there is a question of *representability* [47]: for a given state point, how well can the properties of the underlying polymer system be coherently represented by a single coarse-grained effective pair potential?

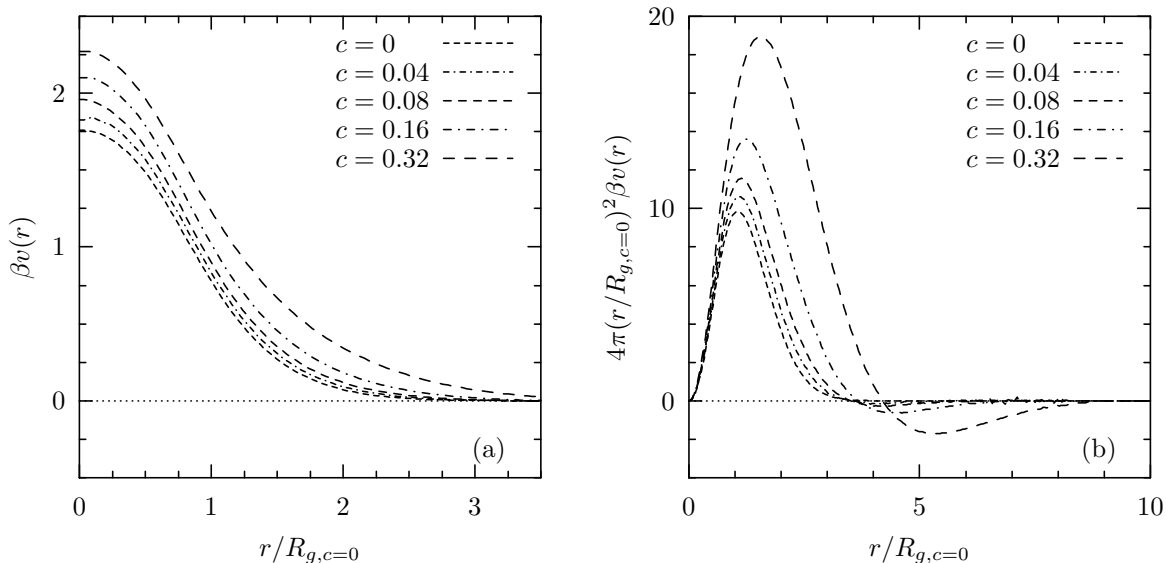


FIG. 7: Effective pair potentials for polymers of length $L = 100$ on the simple cubic lattice at the inverse temperature $\beta = 0.1$ and at various monomer densities c . The x -axis is scaled with the radius of gyration corresponding to $c = 0$ and $\beta = 0.1$.

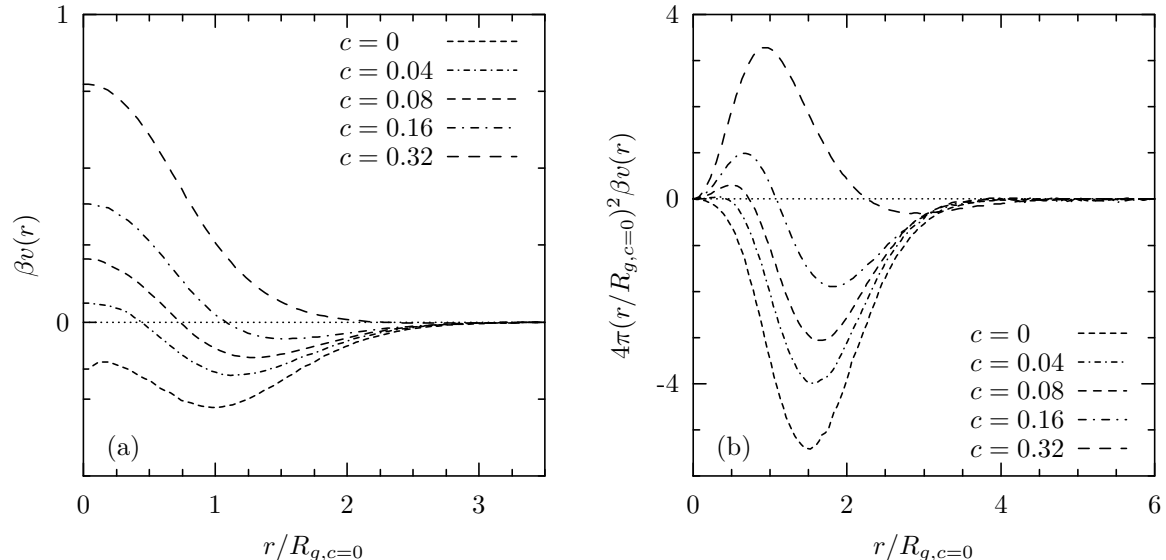


FIG. 8: Effective pair potentials for polymers of length $L = 100$ on the simple cubic lattice at the inverse temperature $\beta = 0.3$ and at various monomer densities c . The x -axis is scaled with the radius of gyration corresponding to $c = 0$ and $\beta = 0.3$.

A. Thermodynamic stability of effective potentials

We briefly repeat the criteria for the existence of a thermodynamic limit described in Ruelle's classic book [38] and valid for state independent interactions. Consider a system of N particles in a volume V . If the total interaction energy V_N , which can be built from pair and higher order terms, satisfies, for all $N > 0$ and for all configurations $\{\mathbf{r}_i\}$ in the configuration space R^N , the inequality

$$V_N(\mathbf{r}_1, \dots, \mathbf{r}_N) \geq -BN \quad (13)$$

with $B \geq 0$, then, according to definition 3.2.1. in Ref. [38], the system is *stable*: the grand partition function converges, and there is a well-defined thermodynamic limit. Potentials that do not satisfy this criterion are termed *catastrophic* by Ruelle. Specializing to pair potentials, i.e.

$$V_N^{(2)}(\mathbf{r}_1, \dots, \mathbf{r}_N) = \sum_{1 \leq i < j \leq N} v_2(|\mathbf{r}_i - \mathbf{r}_j|), \quad (14)$$

condition (13) leads to the following necessary (but not sufficient) condition for the existence of a thermodynamic

limit:

$$\hat{v}(0) = \int v_2(r) 4\pi r^2 dr > 0, \quad (15)$$

which, following Eq. (11), can be rewritten $I_2 > 0$, hence the name “stability” integral for I_2 . If Eq. (15) is not satisfied, then condition (13) can be violated for configurations of a homogeneous fluid. As $N \rightarrow \infty$, the free energy grows super-extensively – the system has no thermodynamic limit – and particles coalesce to form a dense cluster. Condition (15) is necessary, but not sufficient, for the existence of a thermodynamic limit, since one can also construct potentials for which $\hat{v}(0) > 0$, but where the system in a microscopically inhomogeneous (typically, crystalline) state is unstable to coalescence. See Refs. [38] and [30] for explicit examples.

Effective potentials with hard cores, such as those used to describe simple atomic and molecular materials, can be easily shown to satisfy the criterion (13). In contrast, the potentials describing the effective interactions between the CM’s of polymers studied in the present work do not have a hard core, leading to the possibility that two or more “effective” particles occupy the same position in space. The existence of a thermodynamic limit, where the free energy per particle is bounded, is therefore much more subtle.

Although the potentials calculated in this work are state dependent and technically only relevant at the density for which they have been obtained, it is nevertheless interesting to consider what would happen should one of them be used, independently of the density, to describe a system of $N > 2$ particles in a volume V . To this end, we first consider the zero density potentials shown in Fig. 2.

When the underlying SAW polymer system has no nearest-neighbor monomer attractions, the effective pair potentials were shown to be positive [7, 30], so that the criterion (13) is obeyed. However, as Fig. 2 demonstrates, the introduction of nearest-neighbor attractions leads to effective potentials which are no longer positive definite. As the temperature is lowered, the potential grows more and more attractive, until finally it violates the Ruelle criterion and becomes catastrophic. This can be diagnosed in Fig. 4, where I_2 becomes negative at low temperature and the necessary condition (15) is thus violated. In principle, the stability limit of the system should be traced by looking for a state point at which the potential leads to coalescence into microscopically inhomogeneous states, a rather difficult task in general. Here we will use a simpler, approximate criterion, namely Eq. (15), which is a necessary, but not sufficient condition for stability. We will make the heuristic assumption that the true stability limit is not far removed from the simpler one we employ [48]. For a given potential then, Eq. (15) allows us to define the “stability” temperature T_{stab} below which the effective pair potential becomes catastrophic. This explains our nomenclature in Secs. II and III.

The potentials derived at zero density violate Eq. (15) below a temperature $T_{\text{stab}} \approx 3.8$; the potentials are ex-

pected to become unstable to inhomogeneous coalescence at some temperature above that. If one were to use potentials derived for $T \leq T_{\text{stab}}$ at a finite density, the system would be catastrophic.

This naturally leads to the next question: what about the potentials we derived at finite density? There, as shown in Fig. 8, the pair potential can also violate Eq. (15), even though the underlying polymer system is stable, both to coalescence and phase separation, since $T > T_c$ for our $L = 100$ SAW lattice chains. For large enough densities c , the potentials again satisfy Eq. (15).

Serious difficulties are thus emerging with the present coarse-graining procedure: in certain portions of the temperature-density plane, we replace a complex, but perfectly well-behaved, polymer system by a simple soft colloid fluid with pathological thermodynamics! This also raises a certain number of formal concerns. The first one is about the unicity of the mapping between $g(r)$ and $v(r)$ invoked in Sec. IV and demonstrated in Ref. [40]. The theorems rely on well-defined statistical ensembles and their derivations are no longer valid when a catastrophic potential is the outcome of their application. Similarly, the lack of a well defined ensemble also leads to questions about the validity of the liquid state theory, including the Ornstein-Zernike equation, etc.

However, in spite of these formal difficulties, one could take a purely pragmatic attitude: Since it is numerically possible to extract effective pair potentials using the proposed procedure, why not just ignore all the previous concerns and see if these potentials can be of any practical use? To investigate this point, MC simulations of a soft colloid system interacting through the catastrophic effective pair potential obtained for polymers at $\beta = 0.3$ and $c = 0.04$ were performed, revealing a very interesting behavior.

We indeed find that the behavior of the soft colloid fluid depends strongly on the configuration from which the simulation is initiated. When an initial configuration is set up with all soft particles gathered in a single dense cluster, the system coalesces: the particles stay together indefinitely (after a few million MC steps per particle, not a single one has been seen to escape the cluster), and the potential energy per particle e appears unbounded, increasing in absolute value with increasing N ; more precisely, we find $e \simeq -24.6$ for $N = 400$ and $e \simeq -202$ for $N = 3200$, which would give $e(N) \simeq -0.062N$. This is exactly the type of behavior expected from a system interacting through a catastrophic potential. The structure of the clusters also shows distinctive features, as can be seen in Fig. 9, where pair distribution functions $f(r)$ are plotted for the previous cluster sizes. For $N = 3200$, $f(r)$ displays three peaks, located at $r/R_g = 0$, $r/R_g \simeq 1$, and $r/R_g \simeq 1.5$. Quite evidently, the first two peaks originate in the formation of groups of superimposed particles separated by the distance corresponding to the interaction potential minimum. This is indeed a very efficient way for the system to lower its energy, since the energy cost for overlapping particles is modest compared to the

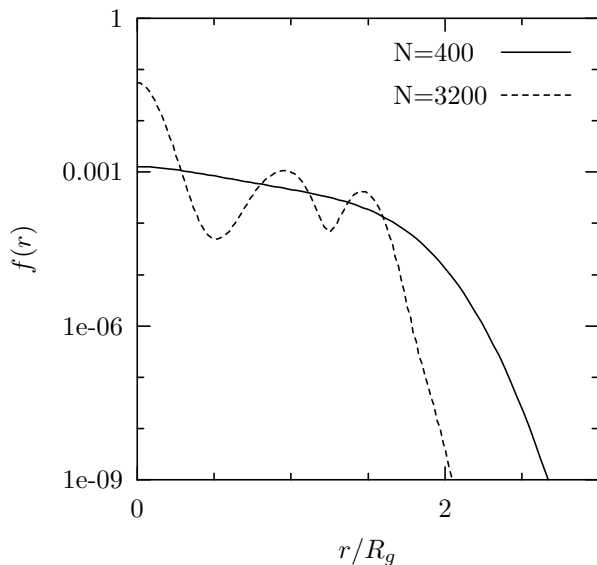


FIG. 9: Pair distribution functions of two collapsed soft colloid systems, with $N = 400$ and $N = 3200$ particles respectively. In both cases, the space integral of $f(r)$ has been normalized to 1 to allow a more significant comparison. The interaction potential is the effective pair potential obtained for a polymer system at $\beta = 0.3$ and $c = 0.04$.

stabilization of pairs of particles at distance $r \simeq R_g$. As for the third peak, it is very likely it has to be associated with the position of the second nearest neighbors. In comparison, for $N = 400$, $f(r)$ is rather featureless and longer-ranged. This change in shape of $f(r)$ is again easily understood from the clustering mechanism. For small N , smaller groups of superimposed particles can be formed, creating less deep energy wells at distance $r \simeq R_g$; the resulting clusters are thus more diffuse and less structured than for large N .

But, if the initial conditions correspond to a homogeneous distribution of particles in the simulation box, the fluid is found to remain homogeneous over the entire time of our simulations (up to 45.10^6 MC steps per particle for 400 particles), suggesting that the homogeneous fluid is metastable with respect to catastrophic coalescence. In this case, the potential energy per particle e is, as expected, independent of the size of the system, i.e. $e \simeq -0.176$ for systems containing 400 or 3200 particles.

Of course, the original polymer system, which is perfectly stable, does not show such a dependence of its behavior on the initial conditions. This can be easily checked by preparing an initial configuration consisting of a dense cluster of polymer chains: the cluster “evaporates” very rapidly, and the density becomes uniform again within a few thousand MC steps per chain only.

In Fig. 10, we compare the $g(r)$ of the metastable fluid phase of the catastrophic soft colloid system to the $g(r)$ of the CM’s of the underlying polymer system at $c = 0.04$ and $\beta = 0.3$. The agreement is excellent! This suggests that the HNC closure used in the inversion procedure,

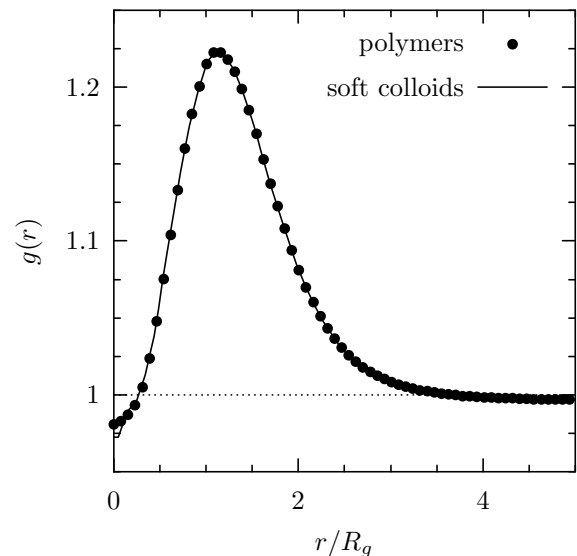


FIG. 10: Comparison of the pair distribution functions obtained from simulations of a polymer system (symbols) and of the corresponding soft colloid fluid in its homogeneous phase (solid line). Here, $\beta = 0.3$, $N = 400$, $L = 100$, $M = 100^3$, and hence $c = 0.04$.

a closure which has been shown to be very accurate for bounded stable potentials [30, 37], still works, in spite of the fact that the potential it produces is catastrophic [49]. The situation is akin to that of the Percus-Yevick solution for the structure of Baxter’s sticky sphere model [26], which is useful for describing hard colloidal systems with very short ranged attractive interactions in spite of the fact that the underlying model system is actually catastrophic [27]. In both cases, the problem is most likely circumvented by the approximate character of the chosen closure.

B. Representability problems for effective potentials

The considerations of the previous section, where the coarse-graining procedure led to catastrophic potentials, are examples of the more general problems of *transferability* and *representability* of effective potentials used to describe complex systems, issues discussed in more detail in a recent review [47].

Transferability problems occur when an effective potential derived at one state point is not applicable at a different state point. In essence all the derived effective potentials in this paper suffer from transferability problems, since they vary with density and with temperature. However, for high temperatures, the density dependence is not that strong, so that the transferability problems are not as important as they appear to be at lower temperatures. For example, the effective potentials in Fig. 8 vary much more rapidly with density, suggesting that one must be very careful in using a potential derived at one

state point as an approximate one for another state point.

Representability problems occur when effective potentials derived to reproduce one physical property, do not easily describe another physical property [47]. For example, one can calculate the (unique) pair potential $v_g(r)$ that reproduces the homogeneous structure (described by $g(r)$) of a system interacting via a Hamiltonian with pair and triplet interaction terms (similarly to what was done in this paper). If the usual equations for the internal energy or the virial pressure, valid for normal pair potentials, are applied to $v_g(r)$, then the latter thermodynamic quantities are not correctly reproduced. This was pointed out many years ago in the context of simple fluids [50]. The same representability problems were already found for the athermal polymer case [47]. They are expected to be more pronounced when the density dependence is as prominent as in Fig. 8. Moreover, as pointed out in the previous section, even more vexing representability problems occur, because the derived effective potentials can lead to systems without a well-defined thermodynamic limit.

The problems of transferability and representability are more important for inhomogeneous systems. For example, at any interface between two phases, it is not clear which potential should be used. Similarly, for the temperature regime that leads to the catastrophic potentials of the previous section, the apparent metastability of the effective “soft colloid” system allows for the inversions to work for a homogeneous system, but this breaks down if the simulations are started with certain inhomogeneous initial conditions. Using some measure of the local density may be a better path to follow. Taking again the example of Fig. 8, if one were to use a local density dependence, the effective system could be stable against collapse, as the potentials would become more repulsive for higher local densities. This would then more closely resemble the underlying polymer system. However, prescriptions for taking local density dependence into account which are both accurate and tractable are not yet well developed.

A final issue not yet resolved is the possible role of volume terms – contributions to the free-energy which are independent of the particular CM configuration. Their effects on phase behavior can be subtle (see e.g. [41, 42]), and they may appear in certain coarse-graining schemes [51]. For the case of polymers in a good solvent, they were shown to be negligible [7, 42], but that may no longer be the case for poorer solvents.

VI. CONCLUSION

We have extended previous work on a coarse-grained description of polymer solutions in good solvent to increasingly poor solvent conditions by adding nearest-neighbor attractions to the initial lattice SAW model, and gradually lowering the temperature. As in the earlier work [7, 10, 46], an effective pair potential $v(r)$ be-

tween the centers of mass of the linear polymer coils was extracted from the Monte Carlo generated CM-CM pair distribution function $g(r)$, using the HNC closure, which is known to be very accurate in the absence of any hard core repulsion. In the infinite dilution limit, the effective pair potential $v_2(r)$ is close to a Gaussian-shaped repulsion, of amplitude $\beta v_2(0) \approx 2$, at high temperatures (corresponding to the SAW limit), but this amplitude decreases as the inverse temperature β increases; an attractive tail develops and at the lowest temperature investigated in our MC simulations, the effective pair potential is entirely attractive, signalling a tendency of the system to coalesce.

At these low temperatures, severe ergodicity problems arise in the MC simulations, and, in the zero density limit, an overlapping histogram method must be used to extract statistically significant results. The problem worsens with increasing polymer length L , so that our simulations were mostly restricted to $L = 100$.

Increasing the polymer concentration at fixed temperature leads to a “restabilization” of the solution in the sense that the effective pair potential exhibits an increasingly repulsive component as the system is taken from the ultra-dilute to the semi-dilute regime. Even at the lowest temperature investigated ($\beta = 0.3$), the effective pair potential reverts to an almost exclusively repulsive Gaussian-like shape at $c = 0.32$ (which, for these polymers, is close to the melt regime).

The occurrence of strongly attractive and significantly state-dependent effective pair potentials between polymer CM’s raises the question of the thermodynamic stability of systems of particles interacting via such “catastrophic” potentials, and of the appropriateness of the coarse-graining procedure to describe solutions of interacting polymers, which are intrinsically stable, close to the θ temperature. The observation that the effective coarse-grained pair potential $v(r)$ is capable of reproducing the $g(r)$ (derived from monomer scale simulations) despite the catastrophic nature of the pair potential, points to the possible existence of metastable homogeneous states generated by these potentials. These metastable states appear to exhibit proper thermodynamic extensivity properties, and may be stabilized against ultimate coalescence by sufficiently high kinetic barriers. If this is indeed the case, the catastrophic effective pair potentials may still provide a useful coarse-graining tool to describe homogeneous states. Strongly inhomogeneous states, generated by coalescence, lead to widely different local densities, and hence would require the use of effective pair potentials depending on the local density. The fact that the effective pair potential tends to become more repulsive at higher density might provide the stabilizing mechanism for the homogeneous state.

We plan to extend the present work to examine polymer CM density profiles near interfaces, and to extract the osmotic equation of state of polymer solutions as a function of concentration and temperature.

Acknowledgments

VK acknowledges support from the EPSRC under grant number GR/M88839 and AAL acknowledges support from the Isaac Newton Trust, Cambridge, and the Royal Society. We thank Chris Addison for a careful reading of the manuscript.

APPENDIX A: OVERLAPPING HISTOGRAM METHOD FOR THE COMPUTATION OF THE EFFECTIVE POTENTIAL BETWEEN TWO CHAINS

We first introduce a reference system consisting of two polymer chains similar to the original ones, except that the intermolecular interaction does not include an attractive nearest-neighbor contribution. The corresponding effective pair potentials $v_2^{\text{ref}}(r)$ can be efficiently computed with the direct method, since the intermolecular Boltzmann weights can only be either 0 or 1 in this case.

The overlapping distribution method is then used to compute $v_2(r) - v_2^{\text{ref}}(r)$, the free-energy difference between the two original chains, with their CM's constrained to stay at a given distance r , and the two reference chains under the same geometrical constraint. To do so, we need to know for these systems the distribution functions $\pi_{\text{orig}}(r, n_c)$ and $\pi_{\text{ref}}(r, n_c)$, respectively, of the number n_c of intermolecular contacts [52], which, according to the theory of the overlapping distribution method, obey the relation

$$\beta v_2(r) - \beta v_2^{\text{ref}}(r) = \ln \frac{\pi_{\text{orig}}(r, n_c)}{\pi_{\text{ref}}(r, n_c)} + \beta \varepsilon n_c, \quad (\text{A1})$$

where $\varepsilon = -1$ denotes the nearest-neighbor pair attrac-

tion.

These histograms have been computed by sampling in canonical Monte Carlo simulations, for both the original and the reference systems, the ensemble of two chain configurations with CM's at distance r . The elementary move we use is the following. One chain is chosen at random and a pivot move is attempted on it. If no self-overlap, leading to immediate rejection, occurs for this chain, a random position with CM's at distance r is chosen for the modified chain around the other coil. If in this position the two chains overlap, the move is rejected, else it is accepted or rejected according to the standard Metropolis rules depending on the change in total energy.

Examples of the accumulated histograms, together with their combination through formula (A1), are shown in Fig. 11. Clearly, the explicit dependence of the left-hand side of Eq. (A1) on n_c is found to disappear as prescribed by the theory, giving us a good indication of the convergence of the method.

The corresponding zero density pair potentials for polymer chains of length $L = 100$ are shown in Fig. 12, where they are compared to the results obtained with the direct simulation method. $\beta = 0.2$ is the largest value at which the direct method gives smooth and reproducible results and thus has been used as a test case for the overlapping histogram approach: as can be seen on the figure, the curves obtained with both simulation methods are indistinguishable. For larger β 's, the effective pair potentials computed with the direct method display irregularities at small distances, especially apparent for $\beta = 0.3$, and originating in the sampling difficulties mentioned in Sec. III. This is clearly not the case of those obtained with the histogram approach which are perfectly smooth and meet the preceding curves for large enough distances at which sampling problems disappear.

-
- [1] For a review, see K. Kremer, in *Monte Carlo and Molecular Dynamics of Condensed Matter Systems*, edited by K. Binder and G. Ciccoti (SIF, Bologna, 1996).
 - [2] P. G. de Gennes, *Scaling Concepts in Polymer Physics* (Cornell University Press, Ithaca NY, 1979).
 - [3] P. J. Flory and W. R. Krigbaum, *J. Chem. Phys.* **18**, 1086 (1950).
 - [4] A. Y. Grosberg, P. G. Khalatur, and A. R. Khokhlov, *Makromol. Chem. Rapid Commun.* **3**, 709 (1982).
 - [5] O. F. Olaj, W. Lantschbauer, and K. H. Pelinka, *Macromolecules* **13**, 299 (1980).
 - [6] J. Dautenhahn and C. K. Hall, *Macromolecules* **27**, 5399 (1994).
 - [7] A. A. Louis, P. G. Bolhuis, J. P. Hansen, and E. J. Meijer, *Phys. Rev. Lett.* **85**, 2522 (2000); P. G. Bolhuis, A. A. Louis, J. P. Hansen, and E. J. Meijer, *J. Chem. Phys.* **114**, 4296 (2001).
 - [8] B. Krüger, L. Schäfer, and A. Baumgärtner, *J. Phys. France* **50**, 319 (1989).
 - [9] see e.g. J. P. Hansen and I. R. McDonald, *Theory of Simple Liquids, 2nd Ed.* (Academic Press, London, 1986).
 - [10] P. G. Bolhuis and A. A. Louis, *Macromolecules* **35**, 1860 (2002).
 - [11] A. A. Louis, P. G. Bolhuis, E. J. Meijer, and J. P. Hansen, *J. Chem. Phys.* **116**, 10547 (2002).
 - [12] A. A. Louis, P. G. Bolhuis, E. J. Meijer, and J. P. Hansen, *J. Chem. Phys.* **117**, 1893 (2002).
 - [13] P. G. Bolhuis, A. A. Louis, and J. P. Hansen, *Phys. Rev. Lett.* **89**, 128302 (2002).
 - [14] P. Grassberger and R. Hegger, *J. Chem. Phys.* **102**, 6881 (1995).
 - [15] C. H. Bennett, *J. Comput. Phys.* **22**, 245 (1976).
 - [16] D. Frenkel and B. Smit, *Understanding molecular simulations* (Academic Press, 1995).
 - [17] A lattice model has been studied for computational convenience. One can reasonably expect that qualitatively similar results would be obtained for a continuous system, since the properties investigated in this work have a characteristic length scale of the order of R_g and thus should not be too dependent on the microscopic details of the

- model. A comparison of the results of the present work with those of Dautenhahn and Hall [6], though rather limited, seems to confirm this point.
- [18] P. J. Flory, *Principles of Polymer Chemistry* (Cornell University Press, Ithaca NY, 1953).
- [19] B. Li, N. Madras, and A. Sokal, *J. Stat. Phys.* **80**, 661 (1995).
- [20] W. Bruns, *Macromolecules* **17**, 2826 (1984).
- [21] H. Meirovitch and H. A. Lim, *J. Chem. Phys.* **92**, 5144 (1990).
- [22] I. Szleifer, E. M. O'Toole, and A. Z. Panagiotopoulos, *J. Chem. Phys.* **97**, 6802 (1992).
- [23] Q. Yan and J. J. de Pablo, *J. Chem. Phys.* **113**, 5954 (2000).
- [24] P. Grassberger, *Phys. Rev. E* **56**, 3682 (1997).
- [25] H. Frauenkron and P. Grassberger, *J. Chem. Phys.* **107**, 9599 (1997).
- [26] R. J. Baxter, *J. Chem. Phys.* **49**, 2270 (1968).
- [27] G. Stell, *J. Stat. Phys.* **63**, 1203 (1991).
- [28] C. Domb and G. S. Joyce, *J. Phys. C* **5**, 959 (1972); C. Domb, *J. Stat. Phys.* **30**, 425 (1983).
- [29] P. M. Duxbury, S. L. A. de Queiroz, and R. B. Stinchcombe, *J. Phys. A* **17**, 2113 (1984); P. M. Duxbury and S. L. A. de Queiroz, *J. Phys. A* **18**, 661 (1985).
- [30] A. A. Louis, P. G. Bolhuis, and J. P. Hansen, *Phys. Rev. E* **62**, 7961 (2000).
- [31] One can easily recognize that $\langle W(|\mathbf{r}_{AB}| = r; \Gamma_A, \Gamma_B) \rangle$ is the ratio of the partition function of two chains with their CM's constrained to stay at distance r over that of two chains infinitely far apart (which is the square of the single chain partition function), and thus that Eq. (6) is a direct implementation of the definition of $v_2(r)$ as the free energy difference between these two systems. But $\langle W(|\mathbf{r}_{AB}| = r; \Gamma_A, \Gamma_B) \rangle$ can also be shown to be the zero density CM pair distribution function as calculated in the grand-canonical ensemble, evidencing that $v_2(r)$ is also the potential of mean-force between the two coils.
- [32] N. Madras and A. D. Sokal, *J. Stat. Phys.* **50**, 109 (1988).
- [33] B. Widom, *J. Chem. Phys.* **39**, 2802 (1963).
- [34] K. S. Shing and K. E. Gubbins, *Mol. Phys.* **46**, 1109 (1982); **49**, 1121 (1983).
- [35] Such a behavior has been seen in computer simulations, see Ref. [5], and is predicted by the mean-field theory as well, see for instance A. Y. Grosberg and D. V. Kuznetsov, *Macromolecules* **25**, 1991 (1992).
- [36] One difficulty with the $L = 100$ chains is that there is no well-defined semi-dilute regime, as discussed in more detail in [7]. When $(4/3)\pi R_g^3 \rho \approx 1$, the monomer density is already $c \approx 0.1$, so that one rapidly enters into the melt regime.
- [37] A. Lang, C. N. Likos, M. Watzlawek, and H. Löwen, *J. Phys.: Condens. Matter* **12**, 5087 (2000); C. N. Likos, A. Lang, M. Watzlawek, and H. Löwen, *Phys. Rev. E* **63**, 031206 (2001).
- [38] D. Ruelle, *Statistical Mechanics: Rigorous Results*, (W. A. Benjamin, Inc., London, 1969).
- [39] To avoid ambiguity, we use the word coalescence, as in G. Gallavotti, *Statistical Mechanics. A short treatise*, (Springer-Verlag, New York, 1999), to qualify the behavior of systems interacting via catastrophic pair potentials, and reserve the word collapse to refer to the coil-to-globule transition of an isolated polymer chain.
- [40] R. L. Henderson, *Phys. Lett. A* **49**, 197 (1974); J. T. Chayes and L. Chayes, *J. Stat. Phys.* **36**, 471 (1984).
- [41] R. van Roij and J. P. Hansen, *Phys. Rev. Lett.* **79**, 3082 (1997); H. Graf and H. Löwen, *Phys. Rev. E* **57**, 5744 (1998); R. van Roij, M. Dijkstra, and J. P. Hansen, *Phys. Rev. E* **59**, 2010 (1999); M. Dijkstra, R. van Roij, and R. Evans, *Phys. Rev. E* **59**, 5744 (1999).
- [42] C. N. Likos, *Phys. Rep.* **348**, 267 (2001).
- [43] L. Reatto, *Phil. Mag. A* **58**, 37 (1986); L. Reatto, D. Levesque, and J. J. Weis, *Phys. Rev. A* **33**, 3451 (1986).
- [44] G. Zerah and J. P. Hansen, *J. Chem. Phys.* **84**, 2336 (1986).
- [45] A. Milchev, W. Paul, and K. Binder, *J. Chem. Phys.* **99**, 4786 (1993); O. F. Olaj, T. Petrik, and G. Zifferer, *Macromol. Theory Simul.* **6**, 1277 (1997); *J. Chem. Phys.* **107**, 10214 (1997).
- [46] P. G. Bolhuis, A. A. Louis, and J. P. Hansen, *Phys. Rev. E* **64**, 021801 (2001).
- [47] A. A. Louis, *J. Phys.: Condens. Matter* **14**, 9187 (2002).
- [48] The use of the approximate criterion (15) might have a deeper physical meaning. First, it can be seen as a specialization of the general stability criterion to a restricted configuration space from which inhomogeneous, non fluid-like configurations are excluded, motivated by the fact that the original polymer system is always fluid and homogeneous in the conditions of the present study. Similar constructions are often invoked in various fields of liquid state theory, for instance to study systems metastable with respect to crystallization like supercooled liquids or colloids near their putative liquid-gas transition. Second, I_2 and B_2 are similar simple functionals of βv_2 . Now, B_2 is used *universally*, i.e. independently of the details of the molecular structure and of the microscopic interactions, for the characterization of the θ point. The use of I_2 could share this universal character. In this respect, it is interesting to note that in the Domb-Joyce model the coalescence catastrophe of a many polymer system, accompanying the appearance of self-trapping behavior of individual chains, occurs exactly when I_2 vanishes.
- [49] These considerations contrast with the approach of L. J. Root, F. H. Stillinger, and G. E. Washington, *J. Chem. Phys.* **88**, 7791 (1988), who, from the strictly opposite point of view, proposed to use the limited ability of a closure relation to detect the coalescence catastrophe embedded in a given potential as a criterion to evaluate the quality of the corresponding integral equation theory.
- [50] J. A. Barker, D. Henderson, and W. R. Smith, *Mol. Phys.* **17**, 579 (1969); G. Casanova, R. J. Dulla, D. A. Jonah, J. S. Rowlinson, and G. Saville, *Mol. Phys.* **18**, 589 (1970); J. S. Rowlinson, *Mol. Phys.* **52**, 567 (1984); M. A. van der Hoef and P. A. Madden, *J. Chem. Phys.* **111**, 1520 (1999).
- [51] F. H. Stillinger, H. Sakai, and S. Torquato, *J. Chem. Phys.* **117**, 288 (2002).
- [52] In the general theory of the overlapping distribution method, distribution functions for the energy differences between the original and reference systems are needed, but here, with the system at hand and for our choice of the reference, the identity between these energy differences and the number n_c of intermolecular contacts is evident.

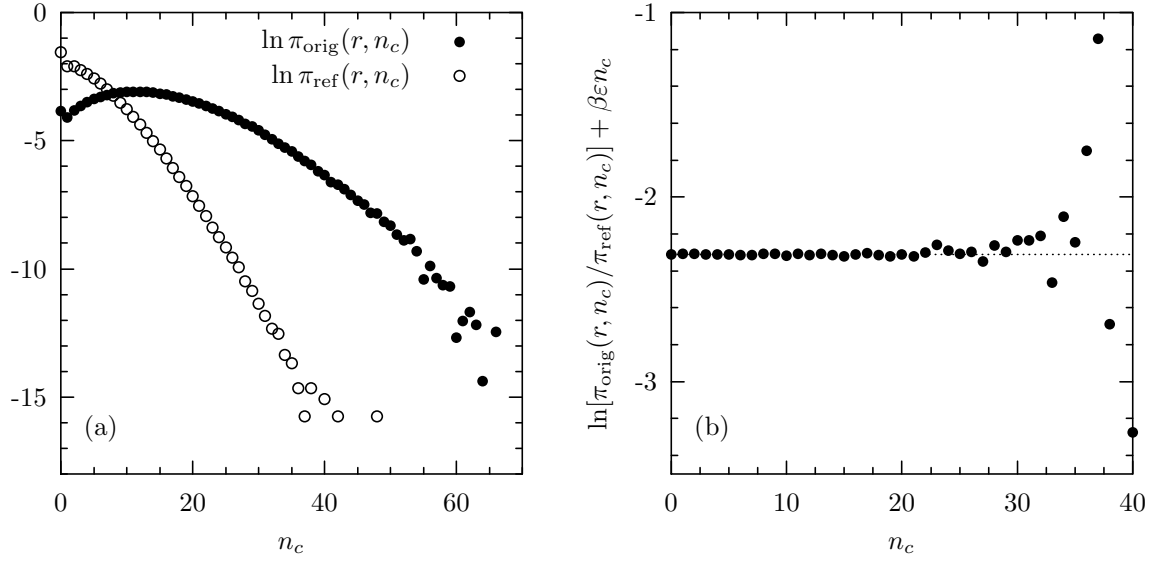


FIG. 11: Distribution functions for the number n_c of intermolecular contacts between two simple cubic lattice chains of length $L = 100$ at $\beta = 0.3$ and with CM's constrained to stay at distance $r = 4.2$. $\pi_{\text{orig}}(r, n_c)$ and $\pi_{\text{ref}}(r, n_c)$ refer to the original and reference systems respectively. (a) Log plot of $\pi_{\text{orig}}(r, n_c)$ and $\pi_{\text{ref}}(r, n_c)$ as functions of n_c . (b) Determination of the free energy difference $v_2(r) - v_2^{\text{ref}}(r)$ using Eq. (A1). As expected from the theory, no explicit dependence of the combination $\ln[\pi_{\text{orig}}(r, n_c)/\pi_{\text{ref}}(r, n_c)] + \beta \epsilon n_c$ on n_c is found.

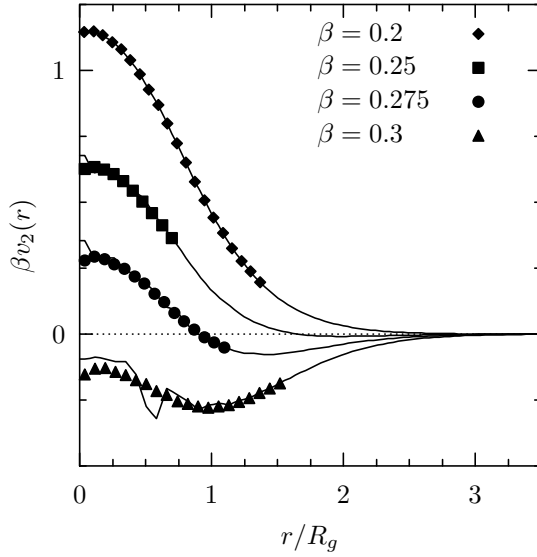


FIG. 12: Comparison of the zero density effective pair potentials obtained with the overlapping histogram method (symbols) and with the direct approach (solid lines) at various inverse temperatures β for polymers of length $L = 100$ on the simple cubic lattice.